Transcriptional acclimation to warming temperatures of the Australian alpine herb *Wahlenbergia ceracea*

Rocco F. Notarnicola[a,b,1], Pieter A. Arnold[a], Zhi-Ping Feng[c], Jemimah Hamilton[a], Ashley W. Jones[a], Stella Loke[d], Adrienne B. Nicotra[a], Benjamin Schwessinger[a], Diep R. Ganguly[a,e,f,1]

[a]Research School of Biology, The Australian National University, Canberra, ACT, 2601, Australia

[b]Evolutionary Biology Group, Faculty of Biology, Adam Mickiewicz University, Poznań, Poland

[c]The John Curtin School of Medical Research, The Australian National University, Canberra, ACT, 2601, Australia

[d]School of Life and Environmental Sciences, Faculty of Science, Deakin University, Geelong, VIC, 3216, Australia

[e]CSIRO Synthetic Biology Future Science Platform, Canberra, ACT, 2601, Australia

[f]Department of Biology, University of Pennsylvania, Philadelphia, PA, 19104, USA

[1]Correspondence: roccofabrizio.notarnicola2@gmail.com, diepganguly@gmail.com

ORCIDs: 0000-0001-9860-6497 (RFN), 0000-0002-6158-7752 (PAA), 0000-0002-7368-1666 (AWJ), 0000-0002-5767-6146 (SL), 0000-0001-6578-369X (ABN), 0000-0002-7194-2922 (BS), 0000-0001-6746-0181 (DRG)

Keywords: thermal tolerance, acclimation, mRNA sequencing, transcription factors, hormone signalling, climate warming, post-transcriptional processes, photosynthesis

Abstract

Understanding the molecular basis of plant heat tolerance helps to predict the consequences of a warming climate on plant performance, particularly in vulnerable environments. Our current understanding comes primarily from studies in *Arabidopsis thaliana* and selected crops exposed to short and intense heat stress. In this study we sought to characterise the molecular responses of an Australian alpine herb (*Wahlenbergia ceracea*) to growth under sustained moderate warming. We compared responses of pre-defined tolerant and sensitive lines, based on measures of photosynthetic stability, to growth under cool or warm temperatures to identify the pathways involved in thermal tolerance and acclimation. Under warmer growth temperatures, *W. ceracea* up-regulated genes involved in RNA metabolism, while down-regulating those involved in photosynthesis and pigment metabolism. In tolerant lines, genes related to photosystem II, light-dependent photosynthetic reactions, and chlorophyll metabolism were more strongly down-regulated. This suggests that the regulation of electron transport and its components may be involved in thermal acclimation. Our results also highlight the importance of hormonal gene networks, particularly ethylene, during longer-term moderate warming. In conclusion, our results point to post-transcriptional processes and the stabilisation of the electron transport chain as candidate mechanisms for thermal acclimation in *W. ceracea*. The study also revealed many non-orthologous temperature-responsive genes, whose characterization may enhance our understanding of physiological acclimation and have relevance for the biotechnological improvement of threatened species and crops.

Introduction

Extreme environments, such as alpine regions, are among those predicted to be most severely impacted by global warming (Gobiet et al., 2014), but native and wild plant species from these environments remain under-represented in genomic studies (Geange et al., 2021). Transcriptomics and bioinformatics have enormous potential to reveal the genomic architecture of traits under selection, their variation, and plasticity and adaptation to climate change (Oomen and Hutchings, 2017; Oomen and Hutchings, 2022); to identify the genetic basis of physiological

attributes and acclimatory responses that may underlie resilience to harsh climates (Rashid et al., 2020); using transcriptomic profiles is likely to yield fundamental advances and potential application for conservation planning (Hansen, 2010; Oomen and Hutchings, 2022). Therefore, application of these techniques to more species and natural populations is warranted.

Plant molecular responses to heat stress have been extensively explored in model plants and crops, such as *Arabidopsis thaliana* and rice (e.g., Niu and Xiang, 2018; Zhang et al., 2021; Li et al., 2021). Transcriptomic studies in *Arabidopsis* and other species revealed that responses to heat involve the regulation of genes encoding proteins collectively known as *heat-shock proteins* (*HSPs*), predominantly chaperones and transcription factors (Richter et al., 2010). The molecular chaperones, such as *HSP70*, *HSP90*, *HSP100*, and *small HSPs* (*sHSPs*), bind unfolded proteins preventing their aggregation and, in some cases, induce their correct re-folding or degradation (Boston et al., 1996; Richter et al., 2010; Wang et al., 2004). The heat-shock transcription factors (*HSFs*) regulate the expression of the *HSPs* in response to many abiotic stresses, including heat (Andrási et al., 2021; Haider et al., 2021a; Haider et al., 2021b). In addition, many phytohormones, such as abscisic acid (ABA) and ethylene, influence the responses to high temperatures (Li et al., 2021). The combination of such molecular responses helps maintain cellular function thereby promoting heat tolerance (Nievola et al., 2017; de Pinto et al., 2015; Yamori et al., 2014).

Most of these studies focus on short, intense heat events, often referred to as heat-shock (Wang et al., 2020), which can be used to infer the pathways that may underlie thermal acclimation. Heat stress causes several changes to the physical and chemical properties inside cells, which in turn affect cellular function. Many proteins and enzymes lose their native folding thus impairing their catalytic function, with decreasing enzymatic activity even at temperatures slightly above their optimum for correct functioning (Daniel et al., 2008; Hobbs et al., 2013); these denatured proteins can form aggregates that eventually kill cells (Goraya et al., 2017; Lippmann et al., 2019). The concentration of reactive oxygen species (ROS) increases during heat stress, causing oxidative damage to proteins, DNA, and lipids (Suzuki and Mittler, 2006). High temperatures also increase membrane fluidity, altering their permeability to water, ions, and solutes, and affecting trans-membrane proteins (Niu and Xiang, 2018; Cano-Ramirez et al., 2021). These changes in membrane stability can directly affect the function of photosystems and photosynthetic reaction centres, located on thylakoid membranes (Hugly et al., 1989).

Experimental heat-shocks may be useful as representations of heatwave events; however, plants also make metabolic and physiological adjustments to optimize their photosynthetic performance under more moderate or prolonged warming (Yamori et al., 2014; Way and Yamori, 2014; Larkindale et al., 2005). Responses to longer-term warming may involve distinct pathways compared to acute responses (Wang et al., 2018; Wang et al., 2020). For example, thermal acclimation to moderate or gradual warming in plants can be achieved by increasing the thermal optimum for photosynthesis, the electron transport rate, and/or stabilising Rubisco activase (Yamori et al., 2014; Way and Yamori, 2014). Thus, it is also vital that we study the molecular responses to longer-term moderate warming that plants must cope with through gradual, sustained rises in average temperature and that we examine these responses in non-model systems.

In this study, we provide *de novo* genome and transcriptome assemblies of the non-model alpine herb *Wahlenbergia ceracea*; we infer orthology with *Arabidopsis thaliana* for thousands of genes, thus providing preliminary annotations; and we investigate differential expression during thermal acclimation to moderate warming, summarising results via enrichment tests and prediction of transcription factors. This species was chosen for study since it demonstrates the capacity to acclimate to warmer growth temperatures, evident through measurable changes in photosynthetic stability (Notarnicola et al., 2021; Arnold et al., 2022), and because we had identified lines that differed significantly in their inherent thermal tolerance. Here, we conducted RNA-sequencing on leaf tissue of sensitive and heat tolerant lines to assess temperature-responsive gene regulation between tolerance categories. We see distinct signatures of regulation of post-transcriptional processes, hormonal (particularly ethylene) signalling, and stabilisation of electron transport chain during thermal acclimation when the sensitive and tolerant lines of this alpine plant are compared.

Materials and Methods

Generation of individuals for mRNA sequencing

Seeds of *W. ceracea* were collected in the field from mature capsules (F0), across the elevation range of the species (1590 – 2095 m a.s.l.) from Charlotte's Pass to Mount Kosciuszko

(NSW, Australia) and subjected to controlled crosses to generate F3 lines (Figure S1). A complete pedigree is presented in Table S1.

To identify tolerant and sensitive lines, we conducted a preliminary experiment where a total of 296 F3 individuals from 37 lines were grown in the glasshouse under cool (24/18°C day/night) or warm (30/25°C day/night) growth temperatures. Heat tolerance was assessed by measuring the temperature-dependent change in chlorophyll fluorescence (T-F_0) as described in Arnold et al. (2021). We ranked lines using their average T_{max} and selected the six F3 lines with the highest and lowest thermal tolerance respectively for the following experiment (tolerant lines average T_{max} = 56.07°C; sensitive lines average T_{max} = 50.83°C; ΔT_{max} [$T_{max/tolerant}$ - $T_{max/sensitive}$] = 5.24°C; Table S2).

Plant growth, temperature treatments and sampling

F3 seeds were germinated in seed raising mix in 14 × 8.5 × 5 cm pots in the glasshouse under 28/20°C to maximise germination and establishment (Notarnicola et al., 2022; Arnold et al., 2022). Subsequently, plants were grown under controlled conditions (28/20°C, 60 % relative humidity, 14-hour photoperiod, 1200 µmol s^{-1} m^{-2}) using a Growth Capsule (Photon Systems Instruments, Brno, Czech Republic). Individual plants were transplanted into individual pots (6.5 × 6.5 × 16 cm) and supplemented with slow-release fertilizer (Osmocote Plus, Scotts Australia). We randomly arranged three replicate plants for each line in three blocks (one replicate per block) that were equivalent in each of 2 capsules. Plants were bottom watered as needed and supplemented with liquid fertiliser every two weeks (Yates Thrive, Yates Australia).

Two weeks after transplantation, plants were subject to either cool (24/15°C day/night, optimal for growth and flowering of post-seedling plants; Arnold et al., 2022) or warm temperatures (30/20°C day/night). Plants grown at 30°C have reduced fitness (seed number and viability) but are not sterile nor undergo photoinhibition [F_v/F_m (maximum PSII efficiency) > 0.70; Notarnicola et al., 2021]. Experimental design: 12 lines × 3 replicates × 2 growth temperatures = 72 individuals (Figure S1). We let the plants grow for a further two weeks by which time they had produced new leaves acclimated to the respective temperature conditions. We took two ~1 mg leaf tissue per plant from the two youngest, fully expanded, healthy leaves. Leaves were harvested in a randomized

order between 11:00 and 16:30, and immediately flash-frozen in liquid nitrogen and stored at -80°C. Time of harvesting and developmental stage were recorded for each sample ('nonflowering' n = 56; 'early bud' n = 16).

Genome annotation and *de novo* transcriptome assembly

DNA was extracted from one F3 individual grown in the glasshouse. High-molecular weight DNA was extracted following Jones et al. (2020) and long-read sequencing was conducted on a PacBio Sequel II platform. We used *Canu HiFi* to assemble the PacBio reads, using a genome size estimate of 0.9 Gb and PacBio HiFi settings (Koren et al. 2017; Nurk et al. 2020). Reads mapping to non-plant contigs were identified using BlobTools and subsequently removed before assembling the remaining reads. Repeats were annotated and masked using RepeatModeler and RepeatMasker (Flynn et al., 2020). Gene annotation was conducted with the BRAKER2 pipeline with flag --epmode (Brůna et al. 2021). Gene predictions were guided by all eudicot orthogroups available in *OrthoDB* v.10 (Kriventseva et al. 2019) and the mRNA sequencing dataset generated herein. For the latter, raw reads across all mRNA-seq samples were merged and aligned to the genome using Subjunc (Liao et al., 2013). The aligned reads were then included in the BRAKER2 predictions. We tested for completeness of the genome assembly and the annotations using Benchmarking Universal Single-Copy Orthologs (*BUSCO*; Seppey et al. 2019). We refer to the predicted gene annotations as the transcriptome.

mRNA-sequencing and analysis

Total RNA was extracted from snap-frozen and ground leaf tissue using the Spectrum™ Plant Total RNA Kit (Merck, Kenilworth, New Jersey, USA) with on-column DNase I digestion. Purified RNA was quality checked for DNA contamination and integrity using semi-denaturing agarose-gel electrophoresis and the LabChip GX Touch (PerkinElmer). RNA was quantified with ND-1000 Spectrophotometer (NanoDrop Technologies) and Qubit 4 Fluorometer (RNA HS kit, Thermo Fisher Scientific).

Library preparation and sequencing were conducted by Deakin Genomics Centre. The construction of cDNA libraries was conducted with 250 ng RNA input using the Illumina stranded mRNA prep ligation protocol, as per manufacturer's instructions except that reaction volumes were scaled by one-half and 12 PCR cycles were used for library amplification (Illumina, San Diego, California, USA). Paired-end sequencing (2 × 150 bp) was conducted on the NovaSeq 6000 (Illumina).

Raw reads were trimmed for adapters and low-quality base calls (PHRED < 20) using *Trim Galore!* (Babraham Bioinformatics) with default settings. Trimmed reads were inspected using *MultiQC* (Ewels et al., 2016), prior to transcript quantification with *Kallisto* (Bray et al., 2016). Quantification was performed on transcripts defined from the *de novo* transcriptome assembly. Transcript abundances were imported into R v.4.0.2 (R Core Team, 2021) and summarised to gene-level counts with *Tximport,* using the 'length scaled transcripts per million (TPM)' equation (Soneson et al., 2015). Only genes detected at > 1 count per million (CPM) in at least 18 samples were retained for analysis. We calculated scaling factors to normalise gene counts based on effective library size using the *calcNormFactors* function in edgeR (Robinson et al., 2010) using the Trimmed Mean of M-values (TMM) method. Differentially expressed genes (DEGs) were identified using the R package 'ThreeDRNAseq' (Guo et al., 2021) and 'limma' algorithms (Smyth, 2004). DEGs were determined using the *limma.pipeline* function in 'ThreeDRNAseq' with Benjamini-Hochberg P-value adjustment (adjusted P-value ≤ 0.05). Initial models included a factor combining the tolerance and temperature factors ('Tolerant_cool', 'Sensitive_cool', 'Tolerant_warm', and 'Sensitive_warm'; n per group = 18), as well as the developmental stage ('nonflowering' and 'early bud'), and collection time. However, preliminary analyses and Principal Component Analysis (PCA) did not reveal clustering of samples by developmental stage nor harvest time and so these factors were not included in the final models. Lines were treated as random effects: within-line correlation was estimated with the *duplicateCorrelation* (Smyth et al., 2005) function in 'limma'. Observational-level and sample-specific quality weights were assigned with the *voomWithQualityWeights* function (Liu et al., 2015). The full model was: gene expression ~ 0 + (tolerance_temperature), random effect = line. The exclusion of the intercept from the model and use of a combined factor allowed us to calculate differences in gene expression between pre-determined contrasts (Table 1).

To explore gene function, we inferred orthogroups between *W. ceracea* and *Arabidopsis thaliana* genes using *OrthoFinder* with default settings (Emms and Kelly, 2019). To improve the phylogenetic inference of orthologs and gene trees, *OrthoFinder* was run with the following proteomes, in addition to those of *W. ceracea* and *A. thaliana*: *Eucalyptus grandis*, *Glycine max*, *Manihot esculenta*, *Oryza sativa*, *Solanum lycopersicum*, *Vitis vinifera*, *Zea mays*, *Chlamidomonas reinardtii*, *Marchantia polymorpha*, *Physcomitrium patens*, and *Selaginella moellendorfii*. *A. thaliana* ortholog TAIR identifiers (Berardini et al., 2015) were used for subsequent analyses (Table 1).

Enrichment tests were performed using *Metascape*. We conducted multi-gene list analyses separately for up- and down-regulated genes to compare enriched terms between tolerant and sensitive lines. These multi-gene lists included orthologs of significant genes in both tolerant and sensitive lines (Table S3, S4). We conducted gene annotation using default terms catalogues, except DrugBank was substituted with KEGG Pathway. We ran enrichment analyses with default settings (catalogues: GO Biological Process, KEGG Pathway, and WikiPathway; minimum overlap = 3; P-value cut-off = 0.01; minimum enrichment factor = 1.5). Transcription factors regulating the DEGs were predicted with *TF2Network* (Kulkarni et al., 2018) on up- and down-regulated genes separately, for tolerant and sensitive lines.

Table 1: Differential gene expression contrasts performed and their biological interpretation. DEGs = differentially expressed genes; Tolerant_warm = tolerant lines grown at warm temperatures; Sensitive_warm = sensitive lines grown at warm temperatures; Tolerant_cool = tolerant lines grown at cool temperatures; Sensitive_cool = sensitive lines grown at cool temperatures.

Contrast	Biological interpretation	Contrast number	total DEGs	Down-regulated DEGs	Up-regulated DEGs	Down-regulated DEGs with orthologs	Up-regulated DEGs with orthologs
(Tolerant_warm + Sensitive_warm) / (Tolerant_cool + Sensitive_cool)	Overall response to temperature	*i*	7,407	3,612	3,795	3,096	2,911
Tolerant_warm - Tolerant_cool	Tolerant lines responses to temperature	*ii*	4,732	2,305	2,427	1,982	1,867
Sensitive_warm - Sensitive_cool	Sensitive lines responses to temperature	*iii*	4,938	2,375	2,563	2,039	1,989

Results

Genome and transcriptome assembly for *Wahlenbergia ceracea*

The size of the haploid genome assembled with *Canu* was 802.965 Mb and accounted for 89% of the estimated genome size (900 Mb). The results for gene space completeness were comparable to other recent, high-quality plant genome assemblies; the assembly reported 91.5% of Embryophyte BUSCOs as complete, and 79.8% of BUSCOs as complete and single copy. However, the assembly recorded low contiguity as the number of contigs was 1876, the contig N50 was 1.125 Mb, and the contig NG50 (based on the estimated genome size) was 0.985. The fragmentation of the genome assembly was related to the presence of repetitive sequences in transposable elements identified at the end of existing contigs. Gene annotations (transcriptome) with BRAKER2 predicted 223,827 exons for 87,730 proteins in the complete assembly. *BUSCO* testing revealed that the transcriptome was overall very similar to the genome assembly, although the former reported a marginal increase in fragmented BUSCOs and a corresponding decrease in complete single copy and missing BUSCOs.

Pseudo-alignment of mRNA-seq reads using Kallisto against the transcripts from the BRAKER2 prediction recovered 41,775 total transcript isoforms, which were summarised to gene-level counts with *Tximport* (Soneson et al., 2015) for a total of 37,307 genes. Of these, 22,585 were considered as expressed (≥ 1 CPM in ≥ 18 samples). On average, 69.7% of reads were pseudo-aligned to the transcriptome per sample (Table S5).

Orthology inference revealed that *W. ceracea* shared the highest number of orthogroups with *Manihot esculenta* (9,357), *Glycine max* (9,275) and *Vitis vinifera* (9,239), among the species used for orthology inference (Table S6). We found 8,854 orthogroups between *W. ceracea* and *Arabidopsis thaliana*, and a total of 11,205 orthologs between the two species (Table S6, S7). Overall, 81.4% (± 0.25 SD) of DEGs (*see below*) were orthologs with *A. thaliana* genes.

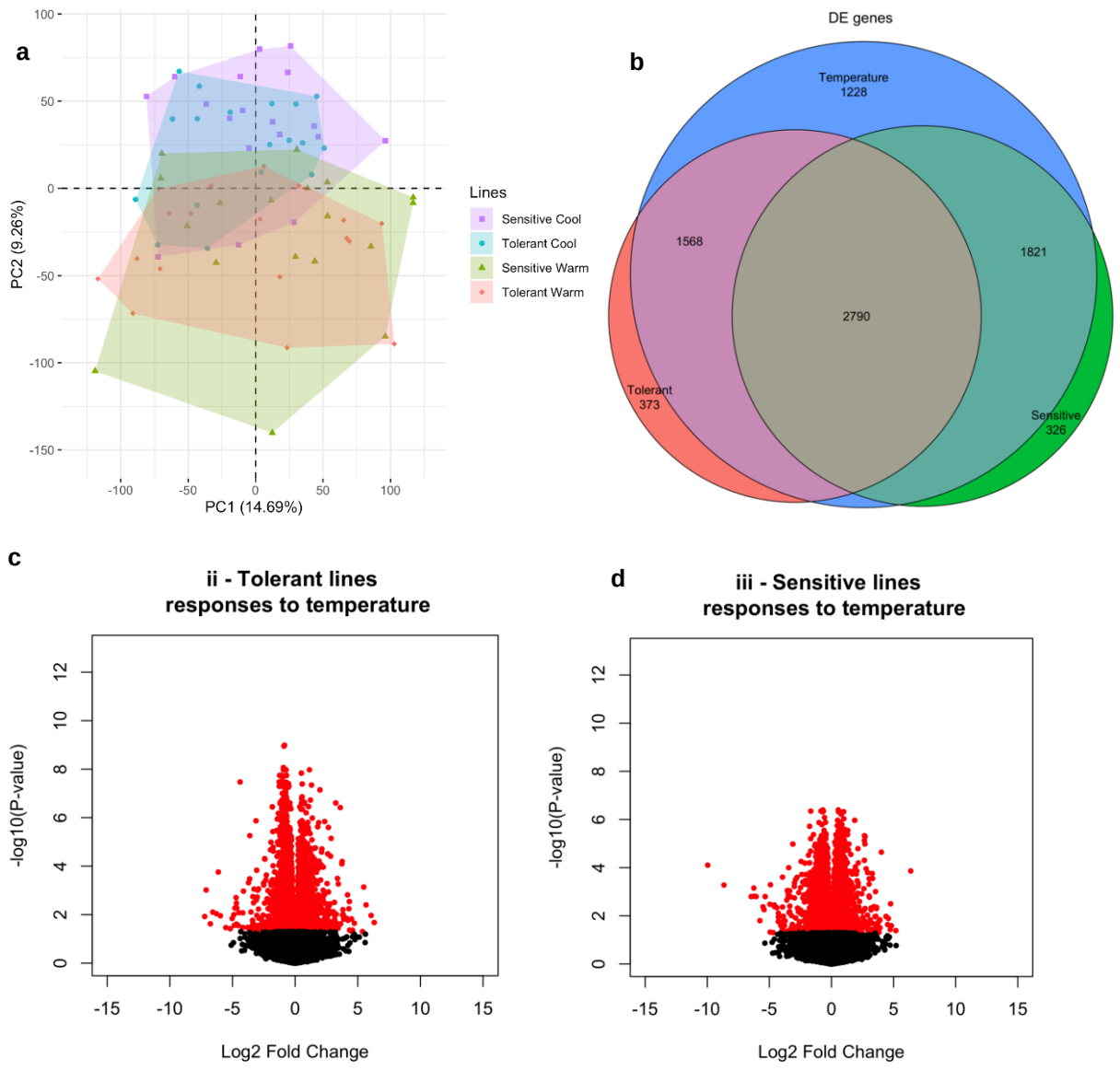

Figure 1: Differential expression analysis reveals separation by temperature treatment along PC2 and highlights overlapping and unique DEGs among tolerance groups. (a) Principal Component Analysis (PCA) on gene expression data between all samples. X-axis = PC1 (14.7%); y-axis = PC2 (9.3%). (b) Venn diagram of shared DEGs between contrasts identified in Table 1: (*i*) (blue), (*ii*) (red), and (*iii*) (green). One DEG significant in contrasts *ii* and *iii* but not in *i* is not shown. (c - d) Volcano plots for contrasts (*ii*) and (*iii*), respectively. X-axis = $\log_2$(fold change expression); y-axis = $-\log_{10}$(P-value). Red dots = DEGs; black dots = non-DEGs.

Tolerant lines of *W. ceracea* display differential regulation of photosynthetic and post-transcriptional processes

Principal Component Analysis (PCA) revealed separation along PC2 (9.26%) reflecting the temperature treatment received (Figure 1a). In contrast, PC1 explained 14.69% of the variation but was not associated with any measured variable and may reflect genetic differences. To ensure we could observe a robust temperature response, we first verified that all *W. ceracea* lines were responsive to warmer conditions (contrast *i*). Indeed, we could detect 7,407 DEGs in response to temperature (Table 1, Figure 1b). Of these, 1,228 were detected when considering all lines (contrast *i*) but were not significant when tested within tolerant or sensitive lines (contrasts *ii* and *iii*) (Figure 1b), presumably due to reduced statistical power with smaller sample sizes. Overall, the results of differential expression and functional enrichment tests in contrast (*i*), presented in Figure S2 and Table S8, recapitulate those in contrasts (*ii*) and (*iii*), therefore we will only report and discuss results for the latter two contrasts.

A total of 4,732 genes (up = 2,305, down = 2,427) and 4,938 genes (up = 2,375, down = 2,563) were differentially expressed in response to temperature in tolerant and sensitive lines, respectively (Table 1). While 2,790 DEGs were in common between tolerance groups, 1,941 and 2,147 were temperature-responsive only in either tolerant or sensitive lines, respectively (Figure 1b). Despite the larger number of DEGs in sensitive lines, responses were more robust in tolerant lines, as shown by the smaller P-values (Figure 1c-d). Fold changes in expression are slightly skewed towards the left, suggesting higher changes in expression for downregulated genes.

In tolerant lines, the most significant upregulated gene in response to temperature did not have orthologs with *A. thaliana* and therefore may represent a novel gene; whereas the second and third genes were orthologs of *bZIP28* (*AT3G10800*; Table S9), a transcription factor upregulated in response to heat that responds to unfolded proteins in the endoplasmic reticulum (Zhang et al., 2017). The most significantly downregulated DEG was ortholog of *AT5G58490* (Table S9), described as a NAD(P)-binding Rossmann-fold superfamily protein. The second and third

downregulated DEGs were orthologs of *Phosphate Transporter 4;1* (*PHT4;1*, *AT2G29650*) localized to the thylakoid membrane and annotated as involved in transmembrane transport.

In sensitive lines, the most significant upregulated gene was an ortholog of *AT4G35785* (Table S10), an RNA binding protein annotated as a positive regulator of mRNA splicing. The second and third top upregulated DEGs were respectively orthologous to *AT4G36420*, described as a ribosomal protein L12, and to *NAP1-related protein* (*NRP2*, *AT1G18800*), a protein that binds to histones and is involved in DNA recombination. The most downregulated gene was an ortholog of *AT5G58490* (Table S7), also found downregulated in tolerant lines. The second and third most significant DEGs were respectively orthologous to *AT2G21960*, encoding a transmembrane protein involved in chlorophyll metabolic process and proteolysis, and to *Vitamin E Deficient 1* (*VTE1*; *AT4G32770*), a cyclase involved in vitamin E synthesis.

To explore the function of temperature-responsive genes, we utilized functional information from orthologous genes in *A. thaliana* determined with OrthoFinder (Emms and Kelly, 2019). A total of 1,790 (upregulated) and 1,975 (downregulated) temperature-responsive genes in tolerant and sensitive lines (combined gene list from contrasts *ii* and *iii*; Tables S6, S7) were recognised and analyzed using Metascape. Overall, up- and down-regulated genes related to post-transcriptional regulation and photosynthesis, respectively (Figure 2a-b). Strikingly, the sensitive lines demonstrated a more significant enrichment of terms related to post-transcriptional regulation of gene expression among the up-regulated genes, such as ribonucleoprotein complex subunit biogenesis and RNA 3'-end processing. The opposite was observed for down-regulated genes, where tolerant lines exhibited a stronger enrichment for various terms including photosynthesis, thylakoid membrane organization, and NAD(P)H dehydrogenase complex assembly.

We next explored expression levels of the photosynthesis-associated DEGs to highlight those genes driving enrichment of this term and potentially involved in the higher T_{max} values observed in tolerant lines. The GO and KEGG term 'photosynthesis' comprised 139 *W. ceracea* DEGs that were orthologs with 89 *A. thaliana* genes. These genes comprised many components of antennae and complexes involved in electron transport, such as two *Protein Phosphatase 1* (*PPH1*), *Light Harvesting Complex A2* (*LHCA2*), *LHCB5*, two *LHCB4.3*, *LHCA2*1*, *LHCB7*, *Oxygen Evolving Complex 33* (*OEC33*), and *ATP synthase C1* (*ATPC1*). All these genes were significant and more down-regulated in tolerant lines, while some of the antennae components were not

significant in sensitive lines (Figure 3). Responses across all lines were consistent with group averages (Figure S3).

The ‘protein folding’ pathway, which includes *HSP*s, was significant among up-regulated genes only in contrast (*i*), but not in contrasts (*ii*) and (*iii*), suggesting no differential regulation between tolerant and sensitive lines. We found nine *HSP*s (five *HSP90s*, one *HSP60*, and three *smallHSP*s) and all were up-regulated under warmer temperatures (Figure S4, S5).

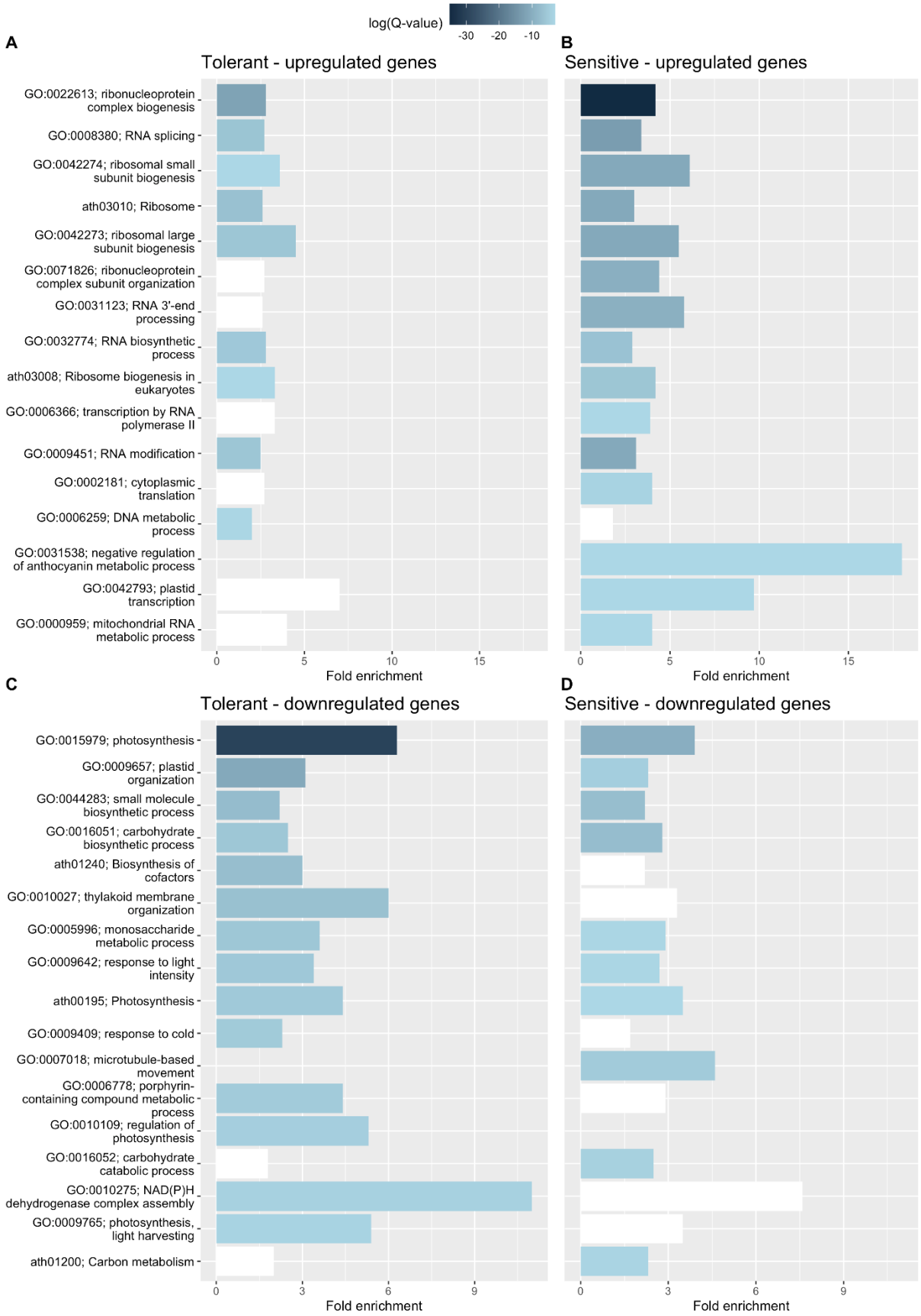
log(Q-value)
-30
-20
-10
A
Tolerant - upregulated genes
GO:0022613; ribonucleoprotein complex biogenesis
GO:0008380; RNA splicing
GO:0042274; ribosomal small subunit biogenesis
ath03010; Ribosome
GO:0042273; ribosomal large subunit biogenesis
GO:0071826; ribonucleoprotein complex subunit organization
GO:0031123; RNA 3'-end processing
GO:0032774; RNA biosynthetic process
ath03008; Ribosome biogenesis in eukaryotes
GO:0006366; transcription by RNA polymerase II
GO:0009451; RNA modification
GO:0002181; cytoplasmic translation
GO:0006259; DNA metabolic process
GO:0031538; negative regulation of anthocyanin metabolic process
GO:0042793; plastid transcription
GO:0000959; mitochondrial RNA metabolic process
0
5
10
15
Fold enrichment
B
Sensitive - upregulated genes
0
5
10
15
Fold enrichment
C
Tolerant - downregulated genes
GO:0015979; photosynthesis
GO:0009657; plastid organization
GO:0044283; small molecule biosynthetic process
GO:0016051; carbohydrate biosynthetic process
ath01240; Biosynthesis of cofactors
GO:0010027; thylakoid membrane organization
GO:0005996; monosaccharide metabolic process
GO:0009642; response to light intensity
ath00195; Photosynthesis
GO:0009409; response to cold
GO:0007018; microtubule-based movement
GO:0006778; porphyrin-containing compound metabolic process
GO:0010109; regulation of photosynthesis
GO:0016052; carbohydrate catabolic process
GO:0010275; NAD(P)H dehydrogenase complex assembly
GO:0009765; photosynthesis, light harvesting
ath01200; Carbon metabolism
0
3
6
9
Fold enrichment
D
Sensitive - downregulated genes
0
3
6
9
Fold enrichment

Figure 2: Tolerant lines exhibited stronger enrichment of photosynthesis-related terms among down-regulated DEGs; sensitive lines had stronger enrichment of post-transcriptional processes among up-regulated DEGs. Bar charts of the significant enriched terms: (a) tolerant lines, upregulated terms; (b) sensitive lines, upregulated terms; (c) tolerant lines, downregulated terms; and (d) sensitive lines, downregulated terms. Significant terms were clustered by *Metascape*; the terms with the highest P-values in each cluster were chosen as representatives. Significant terms are from GO Processes ('GO:…') and KEGG Pathways ('ath…') catalogues. Bars are filled by log(Q-value) calculated for the individual DEG lists (tolerant or sensitive), where Q-value is the adjusted P-value; more negative values (darker bars) correspond to smaller Q-values. Terms are ordered based on their overall Q-values in the combined DEG lists (tolerant + sensitive) in descending order with more significant terms on top. White bars = non-significant terms. X-axis = fold enrichment.

Gene regulatory networks regulating temperature-responsive gene expression in heat tolerant and sensitive *W. ceracea*

Since we observed contrasting regulation between heat tolerant and sensitive *W. ceracea*, we interrogated whether these differences may be the result of transcription factor (TF) activity. Using TF2Network to construct gene regulatory networks, we predicted 47 and 32 TFs from up-regulated temperature-responsive DEGs in tolerant and sensitive lines, respectively, of which 26 were in common (Table S11). Many of the shared TFs predicted for both groups are involved in hormone signalling, particularly with ethylene (numerous *Ethylene-Responsive Factors*) but also chitin, jasmonic acid, cytokinin, and gibberellin. The predicted TFs that were not shared between tolerant and sensitive lines were also involved in ethylene signalling, suggesting a role of this hormone during temperature responses in *W. ceracea*.

Many more TFs were predicted for down-regulated genes; 190 in tolerant and 533 in sensitive lines, with 186 in common between the two groups (Table S11). Among the latter, many TFs were involved in signal transduction during heat stress (e.g., *Heat-Shock Factor 4*, *HSF4*) or in response to hormones, such as abscisic acid, ethylene, and gibberellin. The four TFs predicted only for tolerant lines included two *WRKY TFs* (*WRKY38* and *WRKY26*); whereas the 347 TFs predicted only for sensitive lines revealed enrichments for biosynthetic and developmental (post-embryonic and floral) processes, including ethylene and auxin responses (Figure S6).

We next tested whether any of the identified TFs showed temperature-responsivity in tolerant and sensitive lines. A total of 66 predicted TFs also displayed differential expression in at

least one contrast (Table S11, Figure S7). Among those, two families are also involved in heat responses among their numerous functions: the *bHLH* (seven) and *bZIP* (eight) TF families. We also found significant TFs involved in responses to auxin, responses to ethylene, multicellular organism development, and flower development.

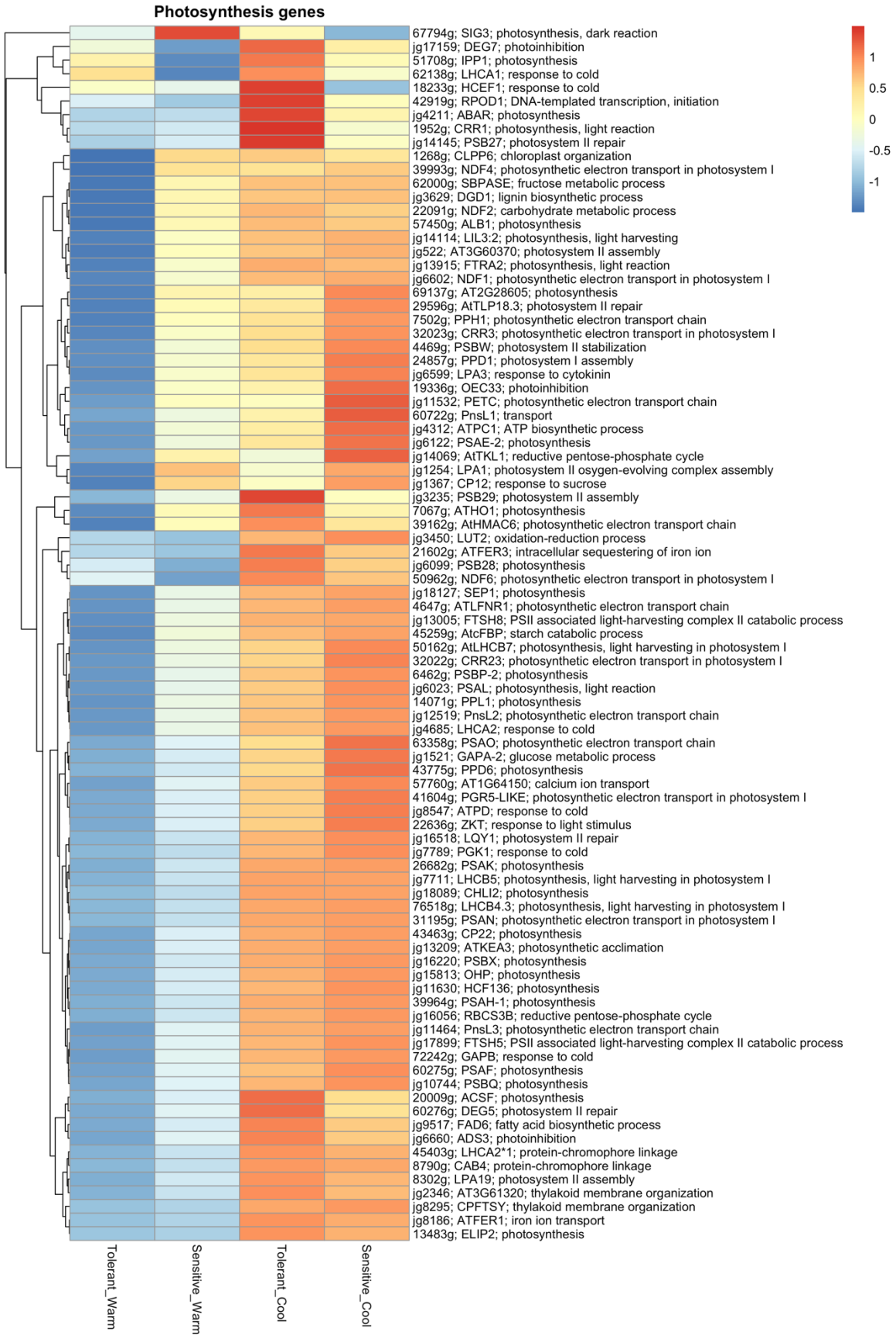
Photosynthesis genes
67794g; SIG3; photosynthesis, dark reaction
jg17159; DEG7; photoinhibition
51708g; IPP1; photosynthesis
62138g; LHCA1; response to cold
18233g; HCEF1; response to cold
42919g; RPOD1; DNA-templated transcription, initiation
jg4211; ABAR; photosynthesis
1952g; CRR1; photosynthesis, light reaction
jg14145; PSB27; photosystem II repair
1268g; CLPP6; chloroplast organization
39993g; NDF4; photosynthetic electron transport in photosystem I
62000g; SBPASE; fructose metabolic process
jg3629; DGD1; lignin biosynthetic process
22091g; NDF2; carbohydrate metabolic process
57450g; ALB1; photosynthesis
jg14114; LIL3:2; photosynthesis, light harvesting
jg522; AT3G60370; photosystem II assembly
jg13915; FTRA2; photosynthesis, light reaction
jg6602; NDF1; photosynthetic electron transport in photosystem I
69137g; AT2G28605; photosynthesis
29596g; AtTLP18.3; photosystem II repair
7502g; PPH1; photosynthetic electron transport chain
32023g; CRR3; photosynthetic electron transport in photosystem I
4469g; PSBW; photosystem II stabilization
24857g; PPD1; photosystem I assembly
jg6599; LPA3; response to cytokinin
19336g; OEC33; photoinhibition
jg11532; PETC; photosynthetic electron transport chain
60722g; PnsL1; transport
jg4312; ATPC1; ATP biosynthetic process
jg6122; PSAE-2; photosynthesis
jg14069; AtTKL1; reductive pentose-phosphate cycle
jg1254; LPA1; photosystem II osygen-evolving complex assembly
jg1367; CP12; response to sucrose
jg3235; PSB29; photosystem II assembly
7067g; ATHO1; photosynthesis
39162g; AtHMAC6; photosynthetic electron transport chain
jg3450; LUT2; oxidation-reduction process
21602g; ATFER3; intracellular sequestering of iron ion
jg6099; PSB28; photosynthesis
50962g; NDF6; photosynthetic electron transport in photosystem I
jg18127; SEP1; photosynthesis
4647g; ATLFNR1; photosynthetic electron transport chain
jg13005; FTSH8; PSII associated light-harvesting complex II catabolic process
45259g; AtcFBP; starch catabolic process
50162g; AtLHCB7; photosynthesis, light harvesting in photosystem I
32022g; CRR23; photosynthetic electron transport in photosystem I
6462g; PSBP-2; photosynthesis
jg6023; PSAL; photosynthesis, light reaction
14071g; PPL1; photosynthesis
jg12519; PnsL2; photosynthetic electron transport chain
jg4685; LHCA2; response to cold
63358g; PSAO; photosynthetic electron transport chain
jg1521; GAPA-2; glucose metabolic process
43775g; PPD6; photosynthesis
57760g; AT1G64150; calcium ion transport
41604g; PGR5-LIKE; photosynthetic electron transport in photosystem I
jg8547; ATPD; response to cold
22636g; ZKT; response to light stimulus
jg16518; LQY1; photosystem II repair
jg7789; PGK1; response to cold
26682g; PSAK; photosynthesis
jg7711; LHCB5; photosynthesis, light harvesting in photosystem I
jg18089; CHLI2; photosynthesis
76518g; LHCB4.3; photosynthesis, light harvesting in photosystem I
31195g; PSAN; photosynthetic electron transport in photosystem I
43463g; CP22; photosynthesis
jg13209; ATKEA3; photosynthetic acclimation
jg16220; PSBX; photosynthesis
jg15813; OHP; photosynthesis
jg11630; HCF136; photosynthesis
39964g; PSAH-1; photosynthesis
jg16056; RBCS3B; reductive pentose-phosphate cycle
jg11464; PnsL3; photosynthetic electron transport chain
jg17899; FTSH5; PSII associated light-harvesting complex II catabolic process
72242g; GAPB; response to cold
60275g; PSAF; photosynthesis
jg10744; PSBQ; photosynthesis
20009g; ACSF; photosynthesis
60276g; DEG5; photosystem II repair
jg9517; FAD6; fatty acid biosynthetic process
jg6660; ADS3; photoinhibition
45403g; LHCA2*1; protein-chromophore linkage
8790g; CAB4; protein-chromophore linkage
8302g; LPA19; photosystem II assembly
jg2346; AT3G61320; thylakoid membrane organization
jg8295; CPFTSY; thylakoid membrane organization
jg8186; ATFER1; iron ion transport
13483g; ELIP2; photosynthesis
Tolerant_Warm
Sensitive_Warm
Tolerant_Cool
Sensitive_Cool
1
0.5
0
-0.5
-1

Figure 3: Heat map of the average expression of the photosynthesis-associated DEGs shows that most of them were more down-regulated in tolerant lines under warming. To ease visualisation, expressions of *W. ceracea* paralogs (orthologs with the same *A. thaliana* ID) were averaged (89 *A. thaliana* IDs). Cells are coloured by Z score. Tolerant_Warm = tolerant lines grown at warm temperatures; Sensitive_Warm = sensitive lines grown at warm temperatures; Tolerant_Cool = tolerant lines grown at cool temperatures; Sensitive_Cool = sensitive lines grown at cool temperatures. Labels on the right show respectively *W. ceracea* gene IDs, *A. thaliana* gene symbols, and GO Processes.

Discussion

In this study we provided *de novo* genome and transcriptome assemblies of the Australian endemic alpine herb *Wahlenbergia ceracea* and functionally annotated thousands of its genes by orthology with *Arabidopsis thaliana*. We then conducted differential gene expression of thermally tolerant and sensitive lines in response to moderate, prolonged warming to identify candidate genes involved in acclimation and thermal tolerance. Thousands of genes in *W. ceracea* had significant changes in expression in response to temperature. Overall, we found that tolerant lines down-regulated chlorophyll biosynthesis and photosynthesis-related processes, including genes encoding components of the antennae and the electron transport chain when exposed to moderate warming. Below we discuss the importance of these results for acclimation of photosynthetic thermal tolerance and pinpoint knowledge gaps for further investigation.

Down-regulation of photosynthetic processes in thermally tolerant lines of *W. ceracea*

Chlorophyll fluorescence is a widely used technique to evaluate the thermostability of the photosystem (PS) II (Geange et al., 2021). Increases in basal chlorophyll fluorescence (F_0) observed in gradually heated leaves, corresponding to the T_{max} parameter, reflect thylakoid membrane instabilities leading to the discharge of electrons and, therefore, PSII disruption. Less well known are the molecular processes that lead to the acclimation in this parameter observed in many species, including *W. ceracea* (Notarnicola et al., 2021).

Here, tolerant lines, characterised as having higher T_{max} values, responded to warmer conditions by down-regulating genes encoding proteins related to thylakoid membrane

organization, pigment metabolism, and light harvesting reactions. These results are confirmed by the analysis of the expression levels of specific photosynthesis-related genes. Specifically, *OEC33, ATPC1,* and many *LHCA*s and *LHCB*s, among other genes encoding components of the PSII or antenna complexes, had lower expressions in tolerant than sensitive lines. A member of the *FAD* family (*FAD6*), involved in membrane desaturation in response to temperature, was also downregulated in tolerant lines. These results suggest that part of acclimation to warmer temperatures may include the downregulation of electron transport from PSII. This is considered a photoprotective mechanism to avoid PSI photoinhibition, which impairs photosynthetic assimilation and photoprotection (Zivcak et al., 2015; Jiang et al., 2021). Under heat-stress, the over-reduction of the electron transport chain is compensated by the cyclic electron transport around PSI (Wang et al., 2006; Rumeau et al., 2007; Jiang et al., 2021). Interestingly though, in our study the genes participating in the NAD(P)H dehydrogenase complex assembly, involved in one of two pathways that generate the cyclic electron transport, were down-regulated in tolerant lines but not in sensitive lines.

In tolerant lines we also found a downregulation of the synthesis of chlorophyll and other pigments. This result is partly in agreement with Wang et al. (2018), which conducted whole-transcriptome sequencing on heat-tolerant strains of *Pyropia haitanensis* exposed to heat stress of several durations, from short-term (a few hours) to long-term (up to six days). However, in Wang et al. (2018) the proportion of downregulated genes related to pigment metabolism decreased with increased heat stress durations. It was proposed that the degradation of photosynthetic pigments and the control of their synthesis may represent physiological mechanisms to reduce the generation of phototoxic intermediates from these compounds during over-excitation (Hörtensteiner, 2006; Wang et al., 2018; Hu et al., 2020). Taken together, these results suggest that photosynthetic thermal tolerance is achieved via conservative reductions of PSII over-excitation and phototoxic damage even at moderately warmer temperatures.

We expected that *HSP*s would play important roles in the acclimation and thermal tolerance of warmer temperatures but while the ‘protein folding’ pathway, which includes the activity of *HSP* chaperones, was significant in overall responses to temperature, we did not observe differences in its regulation between tolerant and sensitive lines.

Prediction of transcription factors reveal possible upstream regulators of thermal acclimation in *W. ceracea*

Transcription factors (TFs) are proteins that mediate the regulation of gene expression by binding the DNA in regulatory regions upon perception of stress or hormonal signals (Meshi and Iwabuchi, 1995; Haider et al., 2021a). Therefore, predicting the TFs governing expression of DEGs allowed us to evaluate the potential upstream regulators and signals involved in thermal tolerance and acclimation.

We found that many DEGs in both tolerant and sensitive lines are regulated, or participate in, ethylene signalling. Several studies (*reviewed in* Poór et al., 2021) demonstrated the involvement of ethylene in plant responses to heat stress through regulation of *HSFs* and *HSPs*. For example, in Wu and Yang (2019), rice seedlings treated with a precursor of ethylene had higher thermal tolerance, chlorophyll *a* content, and higher expression levels of *HSF1*, *HSF2*, and antioxidant enzymes under heat stress than seedlings not treated with this precursor. Besides few relevant differences, in our study ethylene responses of tolerant and sensitive lines were mostly regulated by similar members of the *ERF* family. Future targeted studies of the TFs that do differ between tolerant and sensitive lines may reveal the importance of this hormone in acclimation and thermal tolerance. Generally, the roles of ethylene during regulation of responses to warming warrant further investigations in native species.

It is known that ethylene can induce leaf senescence in plants, both under optimal and high temperature conditions (Li et al., 2013; Kim et al., 2020). Therefore, in annual plants, such as *W. ceracea*, and during abiotic stress, this hormone may be involved in systemic responses to increase leaf turn-over and remobilise nutrients from chloroplasts to reproductive organs, seeds, or new leaves (Schippers et al., 2015; Sade et al., 2018). This result agrees with the downregulation of photosynthetic components mentioned above and the higher investment in flowers and growth observed in *W. ceracea* under warmer temperatures (Notarnicola et al., 2021).

Many DEGs in our study were regulated by other phytohormones, such as cytokinin and jasmonic acid, suggesting these may also be involved in thermal acclimation in *W. ceracea*. Cytokinins promote production of some osmolytes (involved in the detoxification of free radicals), stomata opening, and acclimation during heat stress (Dobrá et al., 2015; Escandón et al., 2016;

Sharma et al., 2019). During prolonged warming, these hormonal pathways may regulate reactive oxygen species (ROS). Indeed, in our study the enzymatic scavengers commonly found after heat-shock, such as *APX*s and *Catalases* were not differentially expressed, except for a *stromal Ascorbate Peroxidase* (*sAPX*) that was significant in all three contrasts (Table S8-S10). The downstream genes and pathways targeted and regulated by phytohormones differ between species and environments, therefore these should be investigated further in *W. ceracea* and other native species during heat stress.

Interestingly, we did not identify any *Heat-Shock Factors* (*HSF*s) regulating temperature-responsive DEGs in this study, nor were *HSF*s differentially regulated (only exceptions were *HSF4*, predicted by TF2Network for down-regulated DEGs of tolerant and sensitive lines, and *HSFB4*, down-regulated in contrast *i*). Instead, other TF families, i.e., *bZIPs* and *bHLHs*, were differentially regulated and predicted, particularly in tolerant lines, suggesting they may be involved in acclimation and thermal tolerance. This result is consistent with Wang et al. (2020) in *Arabidopsis*, where *HSFs* are differentially regulated under heat-shock but not under prolonged warming where other TFs, mainly *bZIPs*, are up-regulated. Many *bZIP*s (e.g., *bZIP28*, here strongly upregulated in tolerant lines) regulate responses to heat-shock and other stresses (Zhao et al., 2020; Haider et al., 2021a; Jing et al., 2022) and respond to abscisic acid (Kim et al., 2004; Skubacz et al., 2016; Dixit et al., 2018), a hormone involved in several functions during heat stress, such as induction of antioxidants and regulation of *HSP*s (Li et al., 2021). Instead, *bHLH*s were down-regulated in our study, consistently with their functions in cool conditions (Sun et al., 2018).

RNA regulation and post-transcriptional processes in native plants

Post-transcriptional regulation indicates a variety of chemical reactions that control the quantity and quality of mRNA molecules (Mazzucotelli et al., 2008; Guerra et al., 2015). A pivotal role in these processes is played by ribonucleoprotein complexes that are involved in splicing, i.e., the removal of introns and the re-arrangement of exons to generate diverse transcripts from one gene sequence (Mazzucotelli et al., 2008; Guerra et al., 2015), or control mRNA decay to ensure transcript turnover (operated by stress granules and processing bodies; Perea-Resa et al., 2016;

Chantarachot and Bailey-Serres, 2018; Kawa et al., 2020). These processes interact with other regulatory mechanisms, such as protein modifications (post-translational regulation), and then feedback back to gene expression adding several layers of regulation to fine-tune responses during thermal acclimation (Miller et al., 2013; Mazzucotelli et al., 2008; Guerra et al., 2015). However, their investigation in native species remains underrepresented.

Evidence from this study revealed that RNA-related processes and ribonucleoprotein complexes may indeed play significant roles in thermal tolerance. Estravis-Barcala et al. (2021) found similar results when comparing *Nothofagus pumilio*, *A. thaliana* and *Populus tomentosa* responses to heat stress. Splicing or RNA and protein modifications induced by heat stress may result in the production of slightly variable protein with altered activity or thermal stability (Reddy, 2007; Staiger and Brown, 2013). Examples of this were found in Rubisco activase (Scafaro et al., 2019; Degen et al., 2021) and *HSFA2* (Liu et al., 2013). So far, the involvement of these mechanisms in plant heat tolerance was predominantly studied in *Arabidopsis*, but our results indicate native species as potential model systems, where the importance of post-translational and post-transcriptional mechanisms for ecological and evolutionary processes can be pinpointed.

Taken together, our results show that responses that occur under a moderate, longer-term heat exposure align with responses to more acute, extreme conditions, although some differences can be pinpointed. However, we note that key genes involved in responses to prolonged warming may go unnoticed if they are not annotated or do not have orthologs with model species. For example, a small fraction (18.6%) of the DEGs in our study did not have orthologs with *A. thaliana* and may represent novel genes involved in specific responses of *W. ceracea* or may be pseudogenes or non-coding RNAs (lncRNAs) with post-transcriptional functions. A wider application of these techniques and development of genomic resources for native species will therefore increase our ability to detect differences among species and conditions. Ultimately, studying new genes and/or gene variants in more non-model, natural species will enable us to predict responses to climate change and to engineer more resistant crop varieties.

Acknowledgements

This project was supported with the provision of plant growth facilities by the Australian Plant Phenomics Facility and computational infrastructure by the National Computational Infrastructure, both supported under the National Collaborative Research Infrastructure Strategy of the Australian Government. We thank the plant services team at The Australian National University for assistance with plant maintenance. We acknowledge the Centre for Biodiversity Analysis Ecogenomics and Bioinformatics Lab, hosted at The Australian National University, for provision of resources. We thank Tenzin Norzin for helping during experimental design, setting up of experiments, and plant maintenance. We also thank Veronica Briceño and Marcin Adamski for consultation.

This research was supported by the Australian Research Council (DP170101681 to ABN) and the Centre for Biodiversity Analysis. RFN was supported by an International Ph.D. Scholarship. DRG was supported by funding from the CSIRO Synthetic Biology Future Science Platform.

Author Contributions

RFN, ABN, PAA, and DRG designed experiments. RFN conducted the experiment, RNA extractions, bioinformatic and statistical analysis, and wrote the manuscript. ABN and PAA helped during leaf samples harvesting. PAA conducted the chlorophyll fluorescence assays to measure T_{max}. BS and JH conducted DNA extraction, sequencing, and *de novo* assembly of the *Wahlenbergia ceracea* genome. SL performed Illumina-based sequencing. DRG and ZF contributed to bioinformatic and statistical analysis. DRG contributed to RNA extractions. BS and SL contributed ideas to the manuscript. ABN, PAA, and DRG critically revised the manuscript.

References

Andrási, N., Pettkó-Szandtner, A., Szabados, L., 2021. Diversity of plant heat shock factors: regulation, interactions, and functions. Journal of Experimental Botany 72, 1558–1575. https://doi.org/10.1093/jxb/eraa576

Arnold, P.A., Briceño, V.F., Gowland, K.M., Catling, A.A., Bravo, L.A., Nicotra, A.B., 2021. A high-throughput method for measuring critical thermal limits of leaves by chlorophyll imaging fluorescence. Functional Plant Biology 48, 634. https://doi.org/10.1071/FP20344

Arnold, P.A., Wang, S., Catling, A.A., Kruuk, L.E.B., Nicotra, A.B., 2022. Patterns of phenotypic plasticity along a thermal gradient differ by trait type in an alpine plant. Functional Ecology 36, 2412-2428. https://doi.org/10.1111/1365-2435.14128

Atlas of Living Australia (2020). Available online at: https://bie.ala.org.au/species/https://id.biodiversity.org.au/node/apni/2905360 (accessed July, 2020).

Berardini, T. Z., Reiser, L., Li, D., Mezheritsky, Y., Muller, R., Strait, E., Huala, E., 2015. The *Arabidopsis* information resource: making and mining the "gold standard" annotated reference plant genome. Genesis 53, 474-485.

Boston, R.S., Viitanen, P.V., Vierling, E., 1996. Molecular chaperones and protein folding in plants. Plant Molecular Biology 32, 191-222.

Bray, N.L., Pimentel, H., Melsted, P., Pachter, L., 2016. Near-optimal probabilistic RNA-seq quantification. Nature Biotechnology 34, 525–527. https://doi.org/10.1038/nbt.3519

Brůna, T., Hoff, K.J., Lomsadze, A., Stanke, M., Borodovsky, M., 2021. BRAKER2: automatic eukaryotic genome annotation with GeneMark-EP+ and AUGUSTUS supported by a protein database. NAR Genomics and Bioinformatics 3, lqaa108. https://doi.org/10.1093/nargab/lqaa108

Cano-Ramirez, D.L., Carmona-Salazar, L., Morales-Cedillo, F., Ramírez-Salcedo, J., Cahoon, E.B., Gavilanes-Ruíz, M., 2021. Plasma Membrane Fluidity: An Environment Thermal Detector in Plants. Cells 10, 2778. https://doi.org/10.3390/cells10102778

Daniel, R.M., Danson, M.J., Eisenthal, R., Lee, C.K., Peterson, M.E., 2008. The effect of temperature on enzyme activity: new insights and their implications. Extremophiles 12, 51–59. https://doi.org/10.1007/s00792-007-0089-7

de Pinto, M.C., Locato, V., Paradiso, A., De Gara, L., 2015. Role of redox homeostasis in thermo-tolerance under a climate change scenario. Annals of Botany 116, 487–496. https://doi.org/10.1093/aob/mcv071

Degen, G.E., Orr, D.J., Carmo-Silva, E., 2021. Heat-induced changes in the abundance of wheat Rubisco activase isoforms. New Phytologist 229, 1298–1311. https://doi.org/10.1111/nph.16937

Dixit, S. K., Gupta, A., & Senthil-Kumar, M. (2018). Current understanding of regulation of GBF3 under abiotic and biotic stresses and its potential role in combined stress tolerance. In Metabolic Adaptations in Plants During Abiotic Stress (pp. 267-272). CRC Press.

Dobrá, J., Černý, M., Štorchová, H., Dobrev, P., Skalák, J., Jedelský, P.L., Lukšanová, H., Gaudinová, A., Pešek, B., Malbeck, J., Vanek, T., Brzobohatý, B., Vanková, R., 2015. The impact of heat stress targeting on the hormonal and transcriptomic response in Arabidopsis. Plant Science 231, 52–61. https://doi.org/10.1016/j.plantsci.2014.11.005

Emms, D.M., Kelly, S., 2019. OrthoFinder: phylogenetic orthology inference for comparative genomics. Genome Biology 20. https://doi.org/10.1186/s13059-019-1832-y

Escandón, M., Cañal, M.J., Pascual, J., Pinto, G., Correia, B., Amaral, J., Meijón, M., 2016. Integrated physiological and hormonal profile of heat-induced thermotolerance in *Pinus radiata*. Tree Physiol 36, 63–77. https://doi.org/10.1093/treephys/tpv127

Estravis-Barcala, M., Heer, K., Marchelli, P., Ziegenhagen, B., Arana, M.V., Bellora, N., 2021. Deciphering the transcriptomic regulation of heat stress responses in Nothofagus pumilio. PLOS ONE 16, e0246615. https://doi.org/10.1371/journal.pone.0246615

Ewels, P., Magnusson, M., Lundin, S., Käller, M., 2016. MultiQC: summarize analysis results for multiple tools and samples in a single report. Bioinformatics 32, 3047–3048. https://doi.org/10.1093/bioinformatics/btw354

Flynn, J.M., Hubley, R., Goubert, C., Rosen, J., Clark, A.G., Feschotte, C., Smit, A.F., 2020. RepeatModeler2 for automated genomic discovery of transposable element families. PNAS 117, 9451–9457. https://doi.org/10.1073/pnas.1921046117

Geange, S.R., Arnold, P.A., Catling, A.A., Coast, O., Cook, A.M., Gowland, K.M., Leigh, A., Notarnicola, R.F., Posch, B.C., Venn, S.E., Zhu, L., Nicotra, A.B., 2021. The thermal tolerance of photosynthetic tissues: a global systematic review and agenda for future research. New Phytologist 229, 2497–2513. https://doi.org/10.1111/nph.17052

Gobiet, A., Kotlarski, S., Beniston, M., Heinrich, G., Rajczak, J., Stoffel, M., 2014. 21st century climate change in the European Alps—A review. Science of The Total Environment 493, 1138–1151. https://doi.org/10.1016/j.scitotenv.2013.07.050

Goraya, G.K., Kaur, B., Asthir, B., Bala, S., Kaur, G., Farooq, M., 2017. Rapid injuries of high temperature in plants. Journal of Plant Biology 60, 298–305. https://doi.org/10.1007/s12374-016-0365-0

Guo, W., Tzioutziou, N.A., Stephen, G., Milne, I., Calixto, C.P., Waugh, R., Brown, J.W.S., Zhang, R., 2021. 3D RNA-seq: a powerful and flexible tool for rapid and accurate differential expression and alternative splicing analysis of RNA-seq data for biologists. RNA Biology 18, 1574–1587. https://doi.org/10.1080/15476286.2020.1858253

Haider, S., Iqbal, J., Naseer, S., Shaukat, M., Abbasi, B.A., Yaseen, T., Zahra, S.A., Mahmood, T., 2021a. Unfolding molecular switches in plant heat stress resistance: A comprehensive review. Plant Cell Reports. https://doi.org/10.1007/s00299-021-02754-w

Haider, S., Rehman, S., Ahmad, Y., Raza, A., Tabassum, J., Javed, T., Osman, H.S., Mahmood, T., 2021b. In Silico Characterization and Expression Profiles of Heat Shock Transcription Factors (HSFs) in Maize (Zea mays L.). Agronomy 11, 2335. https://doi.org/10.3390/agronomy11112335

Hansen, M.M., 2010. Expression of interest: transcriptomics and the designation of conservation units. Molecular Ecology 19, 1757–1759. https://doi.org/10.1111/j.1365-294X.2010.04597.x

Hobbs, J.K., Jiao, W., Easter, A.D., Parker, E.J., Schipper, L.A., Arcus, V.L., 2013. Change in Heat Capacity for Enzyme Catalysis Determines Temperature Dependence of Enzyme Catalyzed Rates. ACS Chemical Biology 8, 2388–2393. https://doi.org/10.1021/cb4005029

Hörtensteiner, S., 2006. Chlorphyll degradation during senescence. Annual Review Plant Biology 57, 55–77. https://doi.org/10.1146/annurev.arplant.57.032905.105212

Hu, S., Ding, Y., Zhu, C., 2020. Sensitivity and Responses of Chloroplasts to Heat Stress in Plants. Frontiers Plant Science 11, 375. https://doi.org/10.3389/fpls.2020.00375

Hugly, S., Kunst, L., Browse, J., Somerville, C., 1989. Enhanced Thermal Tolerance of Photosynthesis and Altered Chloroplast Ultrastructure in a Mutant of *Arabidopsis* Deficient in Lipid Desaturation. Plant Physiology 90, 1134–1142. https://doi.org/10.1104/pp.90.3.1134

Jiang, Y., Feng, X., Wang, H., Chen, Y., Sun, Y., 2021. Heat-induced down-regulation of photosystem II protects photosystem I in honeysuckle (Lonicera japonica). Journal of Plant Research 134, 1311–1321. https://doi.org/10.1007/s10265-021-01336-x

Jing, Y., Yu, Y., Wang, H., Wu, Y., Li, C., 2022. Genome-wide identification and expression analysis of the bZIP gene family in silver birch (Betula pendula Roth.). Journal of Forestry Research. https://doi.org/10.1007/s11676-022-01453-w

Jones, A., Torkel, C., Borevitz, J., Schwessinger, B., 2020. Scalable high-molecular weight DNA extraction for long-read sequencing. Protocols.io, v1.

Kim, S., Kang, J., Cho, D.-I., Park, J.H., Kim, S.Y., 2004. ABF2, an ABRE-binding bZIP factor, is an essential component of glucose signaling and its overexpression affects multiple stress tolerance: ABF2 is a positive component of glucose signaling. The Plant Journal 40, 75–87. https://doi.org/10.1111/j.1365-313X.2004.02192.x

Kim, C., Kim, S.J., Jeong, J., Park, E., Oh, E., Park, Y.-I., Lim, P.O., Choi, G., 2020. High Ambient Temperature Accelerates Leaf Senescence via PHYTOCHROME-INTERACTING FACTOR 4 and 5 in Arabidopsis. *Molecules and Cells*, *43*, 645

Knight, C.A., Ackerly, D.D., 2002. An ecological and evolutionary analysis of photosynthetic thermotolerance using the temperature-dependent increase in fluorescence. Oecologia 130, 505–514. https://doi.org/10.1007/s00442-001-0841-0

Koren, S., Walenz, B.P., Berlin, K., Miller, J.R., Bergman, N.H., Phillippy, A.M., 2017. Canu: scalable and accurate long-read assembly via adaptive *k* -mer weighting and repeat separation. Genome Research 27, 722–736. https://doi.org/10.1101/gr.215087.116

Kriventseva, E.V., Kuznetsov, D., Tegenfeldt, F., Manni, M., Dias, R., Simão, F.A., Zdobnov, E.M., 2019. OrthoDB v10: sampling the diversity of animal, plant, fungal, protist, bacterial and viral genomes for evolutionary and functional annotations of orthologs. Nucleic Acids Research 47, D807–D811. https://doi.org/10.1093/nar/gky1053

Kulkarni, S.R., Vaneechoutte, D., Van de Velde, J., Vandepoele, K., 2018. TF2Network: predicting transcription factor regulators and gene regulatory networks in Arabidopsis using publicly available binding site information. Nucleic Acids Research 46, e31–e31. https://doi.org/10.1093/nar/gkx1279

Larkindale, J., Hall, J.D., Knight, M.R., Vierling, E., 2005. Heat Stress Phenotypes of Arabidopsis Mutants Implicate Multiple Signaling Pathways in the Acquisition of Thermotolerance. Plant Physiology 138, 882–897. https://doi.org/10.1104/pp.105.062257

Li, N., Euring, D., Cha, J.Y., Lin, Z., Lu, M., Huang, L.-J., Kim, W.Y., 2021. Plant Hormone-Mediated Regulation of Heat Tolerance in Response to Global Climate Change. Frontiers in Plant Science 11, 627969. https://doi.org/10.3389/fpls.2020.627969

Li, Z., Peng, J., Wen, X., Guo, H., 2013. *ETHYLENE-INSENSITIVE3* Is a Senescence-Associated Gene That Accelerates Age-Dependent Leaf Senescence by Directly Repressing *miR164* Transcription in *Arabidopsis*. The Plant Cell 25, 3311–3328. https://doi.org/10.1105/tpc.113.113340

Liao, Y., Smyth, G.K., Shi, W., 2013. The Subread aligner: fast, accurate and scalable read mapping by seed-and-vote. Nucleic Acids Research 41, e108–e108. https://doi.org/10.1093/nar/gkt214

Lippmann, R., Babben, S., Menger, A., Delker, C., Quint, M., 2019. Development of Wild and Cultivated Plants under Global Warming Conditions. Current Biology 29, R1326–R1338. https://doi.org/10.1016/j.cub.2019.10.016

Liu, J., Sun, N., Liu, M., Liu, J., Du, B., Wang, X., Qi, X., 2013. An Autoregulatory Loop Controlling Arabidopsis *HsfA2* Expression: Role of Heat Shock-Induced Alternative Splicing. Plant Physiology 162, 512–521. https://doi.org/10.1104/pp.112.205864

Liu, R., Holik, A.Z., Su, S., Jansz, N., Chen, K., Leong, H.S., Blewitt, M.E., Asselin-Labat, M.-L., Smyth, G.K., Ritchie, M.E., 2015. Why weight? Modelling sample and observational level variability improves power in RNA-seq analyses. Nucleic Acids Research 43, e97–e97. https://doi.org/10.1093/nar/gkv412

Meshi, T., Iwabuchi, M., 1995. Plant transcription factors. Plant and cell physiology 36, 1405-1420.

Nievola, C.C., Carvalho, C.P., Carvalho, V., Rodrigues, E., 2017. Rapid responses of plants to temperature changes. Temperature 4, 371–405. https://doi.org/10.1080/23328940.2017.1377812

Niu, Y., Xiang, Y., 2018. An Overview of Biomembrane Functions in Plant Responses to High-Temperature Stress. Frontiers in Plant Science 9, 915. https://doi.org/10.3389/fpls.2018.00915

Notarnicola, R.F., Nicotra, A.B., Kruuk, L.E.B., Arnold, P.A., 2021. Tolerance of Warmer Temperatures Does Not Confer Resilience to Heatwaves in an Alpine Herb. Frontiers in Ecology and Evolution 9. https://doi.org/10.3389/fevo.2021.615119

Notarnicola, R.F., Nicotra, A.B., Kruuk, L.E.B. and Arnold, P.A., 2022. Effects of warming temperatures on germination responses and trade-offs between seed traits in an alpine plant. Journal of Ecology.

Nurk, S., Walenz, B.P., Rhie, A., Vollger, M.R., Logsdon, G.A., Grothe, R., Miga, K.H., Eichler, E.E., Phillippy, A.M., Koren, S., 2020. HiCanu: accurate assembly of segmental duplications, satellites, and allelic variants from high-fidelity long reads. Genome Research 30, 1291–1305. https://doi.org/10.1101/gr.263566.120

Oomen, R.A., Hutchings, J.A., 2022. Genomic reaction norms inform predictions of plastic and adaptive responses to climate change. Journal of Animal Ecology 91, 1073–1087. https://doi.org/10.1111/1365-2656.13707

Oomen, R.A., Hutchings, J.A., 2017. Transcriptomic responses to environmental change in fishes: Insights from RNA sequencing. FACETS 2, 610–641. https://doi.org/10.1139/facets-2017-0015

Poór, P., Nawaz, K., Gupta, R., Ashfaque, F., Khan, M.I.R., 2021. Ethylene involvement in the regulation of heat stress tolerance in plants. Plant Cell Reports. https://doi.org/10.1007/s00299-021-02675-8

R Core Team (2021). R: A language and environment for statistical computing. R Foundation for Statistical Computing, Vienna, Austria. URL https://www.R-project.org/.

Rashid, F.A.A., Crisp, P.A., Zhang, Y., Berkowitz, O., Pogson, B.J., Day, D.A., Masle, J., Dewar, R.C., Whelan, J., Atkin, O.K., Scafaro, A.P., 2020. Molecular and physiological responses during thermal acclimation of leaf photosynthesis and respiration in rice. Plant, Cell & Environment 43, 594–610. https://doi.org/10.1111/pce.13706

Reddy, A.S.N., 2007. Alternative Splicing of Pre-Messenger RNAs in Plants in the Genomic Era. Annu. Rev. Plant Biol. 58, 267–294. https://doi.org/10.1146/annurev.arplant.58.032806.103754

Richter, K., Haslbeck, M., Buchner, J., 2010. The Heat Shock Response: Life on the Verge of Death. Molecular Cell 40, 253–266. https://doi.org/10.1016/j.molcel.2010.10.006

Robinson, M.D., McCarthy, D.J., Smyth, G.K., 2010. edgeR: a Bioconductor package for differential expression analysis of digital gene expression data. Bioinformatics 26, 139-140. https://doi.org/10.1093/bioinformatics/btp616

Rumeau, D., Peltier, G., Cournac, L., 2007. Chlororespiration and cyclic electron flow around PSI during photosynthesis and plant stress response. Plant, Cell & Environment 30, 1041–1051. https://doi.org/10.1111/j.1365-3040.2007.01675.x

Sade, N., Del Mar Rubio-Wilhelmi, M., Umnajkitikorn, K., Blumwald, E., 2018. Stress-induced senescence and plant tolerance to abiotic stress. Journal of Experimental Botany 69, 845–853. https://doi.org/10.1093/jxb/erx235

Scafaro, A.P., Bautsoens, N., den Boer, B., Van Rie, J., Gallé, A., 2019. A Conserved Sequence from Heat-Adapted Species Improves Rubisco Activase Thermostability in Wheat. Plant Physiology 181, 43–54. https://doi.org/10.1104/pp.19.00425

Schippers, J.H.M., Schmidt, R., Wagstaff, C., Jing, H.-C., 2015. Living to Die and Dying to Live: The Survival Strategy behind Leaf Senescence. Plant Physiol. 169, 914–930. https://doi.org/10.1104/pp.15.00498

Seppey, M., Manni, M. and Zdobnov, E.M., 2019. BUSCO: assessing genome assembly and annotation completeness. In Gene prediction (pp. 227-245). Humana, New York, NY.

Sharma, A., Shahzad, B., Kumar, V., Kohli, S.K., Sidhu, G.P.S., Bali, A.S., Handa, N., Kapoor, D., Bhardwaj, R., Zheng, B., 2019. Phytohormones Regulate Accumulation of Osmolytes Under Abiotic Stress. Biomolecules 9, 285. https://doi.org/10.3390/biom9070285

Skubacz, A., Daszkowska-Golec, A., Szarejko, I., 2016. The Role and Regulation of ABI5 (ABA-Insensitive 5) in Plant Development, Abiotic Stress Responses and Phytohormone Crosstalk. Frontiers in Plant Science 7. https://doi.org/10.3389/fpls.2016.01884

Smyth, G.K., 2004. Linear Models and Empirical Bayes Methods for Assessing Differential Expression in Microarray Experiments. Statistical Applications in Genetics and Molecular Biology 3, 1–25. https://doi.org/10.2202/1544-6115.1027

Smyth, G.K., Michaud, J., Scott, H.S., 2005. Use of within-array replicate spots for assessing differential expression

in microarray experiments. Bioinformatics 21, 2067–2075. https://doi.org/10.1093/bioinformatics/bti270

Soneson, C., Love, M.I., Robinson, M.D., 2015. Differential analyses for RNA-seq: transcript-level estimates improve gene-level inferences. F1000 Research 4, 1521. https://dx.doi.org/10.12688%2Ff1000research.7563.2

Staiger, D., Brown, J.W.S., 2013. Alternative Splicing at the Intersection of Biological Timing, Development, and Stress Responses. Plant Cell 25, 3640–3656. https://doi.org/10.1105/tpc.113.113803

Sun, X., Wang, Y., Sui, N., 2018. Transcriptional regulation of bHLH during plant response to stress. Biochemical and Biophysical Research Communications 503, 397–401. https://doi.org/10.1016/j.bbrc.2018.07.123

Suzuki, N., Mittler, R., 2006. Reactive oxygen species and temperature stresses: A delicate balance between signaling and destruction. Physiologia Plantarum 126, 45–51. https://doi.org/10.1111/j.0031-9317.2005.00582.x

Wang, L., Ma, K.-B., Lu, Z.-G., Ren, S.-X., Jiang, H.-R., Cui, J.-W., Chen, G., Teng, N.-J., Lam, H.-M., Jin, B., 2020. Differential physiological, transcriptomic and metabolomic responses of Arabidopsis leaves under prolonged warming and heat shock. BMC Plant Biol 20, 86. https://doi.org/10.1186/s12870-020-2292-y

Wang, P., Duan, W., Takabayashi, A., Endo, T., Shikanai, T., Ye, J.Y., Mi, H., 2006. Chloroplastic NAD(P)H Dehydrogenase in Tobacco Leaves Functions in Alleviation of Oxidative Damage Caused by Temperature Stress. Plant Physiology 141, 465–474. https://doi.org/10.1104/pp.105.070490

Wang, W., Teng, F., Lin, Y., Ji, D., Xu, Y., Chen, C., Xie, C., 2018. Transcriptomic study to understand thermal adaptation in a high temperature-tolerant strain of Pyropia haitanensis. PLoS ONE 13, e0195842. https://doi.org/10.1371/journal.pone.0195842

Wang, W., Vinocur, B., Shoseyov, O., Altman, A., 2004. Role of plant heat-shock proteins and molecular chaperones in the abiotic stress response. Trends in Plant Science 9, 244–252. https://doi.org/10.1016/j.tplants.2004.03.006

Way, D.A., Yamori, W., 2014. Thermal acclimation of photosynthesis: on the importance of adjusting our definitions and accounting for thermal acclimation of respiration. Photosynthesis Research 119, 89–100. https://doi.org/10.1007/s11120-013-9873-7

Wu, Y.-S., Yang, C.-Y., 2019. Ethylene-mediated signaling confers thermotolerance and regulates transcript levels of heat shock factors in rice seedlings under heat stress. Botanical Studies 60, 23. https://doi.org/10.1186/s40529-019-0272-z

Yamori, W., Hikosaka, K., Way, D.A., 2014. Temperature response of photosynthesis in C3, C4, and CAM plants: temperature acclimation and temperature adaptation. Photosynthesis Research 119, 101–117. https://doi.org/10.1007/s11120-013-9874-6

Zhang, H., Zhu, J., Gong, Z., Zhu, J.-K., 2021. Abiotic stress responses in plants. Nature Reviews Genetics. https://doi.org/10.1038/s41576-021-00413-0

Zhang, S.-S., Yang, H., Ding, L., Song, Z.-T., Ma, H., Chang, F., Liu, J.-X., 2017. Tissue-Specific Transcriptomics Reveals an Important Role of the Unfolded Protein Response in Maintaining Fertility upon Heat Stress in Arabidopsis. Plant Cell 29, 1007–1023. https://doi.org/10.1105/tpc.16.00916

Zhao, J., Lu, Z., Wang, L., Jin, B., 2020. Plant Responses to Heat Stress: Physiology, Transcription, Noncoding RNAs, and Epigenetics. IJMS 22, 117. https://doi.org/10.3390/ijms22010117

Zivcak, M., Brestic, M., Kunderlikova, K., Sytar, O., Allakhverdiev, S.I., 2015. Repetitive light pulse-induced photoinhibition of photosystem I severely affects CO2 assimilation and photoprotection in wheat leaves. Photosynthesis Research 126, 449–463. https://doi.org/10.1007/s11120-015-0121-1